A Performance Study of Spatial Modulation Systems Under Vehicle-to-Vehicle Channel Models

Yu Fu[1], Cheng-Xiang Wang[2,1], Raed Mesleh[3], Xiang Cheng[4], Harald Haas[5], and Yejun He[6]
[1]Joint Research Institute for Signal and Image Processing, Heriot-Watt University, Edinburgh, EH14 4AS, UK.
[2]School of Information Science and Engineering, Shandong University, Jinan, 250100, China.
[3]Electrical Engineering Department and SNCS Research Center, University of Tabuk, P.O.Box: 741, 71491, Tabuk, Saudi Arabia.
[4]School of Electronics Engineering & Computer Science, Peking University, Beijing, 100871, China.
[5]Joint Research Institute for Signal and Image Processing, University of Edinburgh, Edinburgh, EH9 3JL, UK.
[6]College of Information Engineering, Shenzhen University, Shenzhen, 518060, China.
Email: {yf54, cheng-xiang.wang}@hw.ac.uk, rmesleh.sncs@ut.edu.sa, xiangcheng@pku.edu.cn, h.haas@ed.ac.uk, yjhe@szu.edu.cn

***Abstract*—Spatial modulation (SM) is a relatively new multiple-input multiple-output (MIMO) technology that can provide high data rate with reasonable spectral efficiency. In this paper, the bit error rate (BER) performance of SM systems under vehicle-to-vehicle (V2V) channel models is investigated. The theoretical BER expression is given. The impact of some V2V channel model parameters on the underlying space-time correlation function (STCF) and the BER performance of SM systems are also studied. Simulation results indicate that modulation schemes, maximum Doppler frequency, the distance between the transmitter (Tx) and receiver (Rx), and antenna element spacings can affect the performance of SM systems.**

***Keywords* – Spatial modulation, vehicle-to-vehicle channel model, bit error rate, space-time correlation function.**

I. Introduction

The MIMO technology has been widely used in modern wireless communication systems to improve the data rate and system reliability [1], [2]. In general, MIMO technologies can be classified into following categories: spatial multiplexing where multiple independent streams are transmitted through different antennas at the same time and on the same frequency [3]. The Bell Labs layered space-time architecture (BLAST) is a typical example of spatial multiplexing, which was first introduced by Foschini *et al.* in [4]. Space-time-coding (STC) is the second category which transmit the same stream from different antennas to increase transmission reliability. The Alamouti scheme is a typical example of this category [5]. The third category of MIMO technologies assumes the knowledge of the channel's information at both the Tx and Rx. The signal is transmitted with the decomposed product of the channel matrix to achieve capacity gain [5]. Beamforming is a typical technology of this category. However, these MIMO technologies suffer from disadvantages such as the high receiver complexity and the inter-channel interference (ICI) problem. Thus, SM was proposed in [5] to overcome some of these limitations by maintaining multiplexing gain while at the same time entirely avoiding ICI.

In SM, only one transmit antenna is active at each time instant. The index of the transmit antenna becomes an important resource to carry information that is utilized to increase spectral efficiency [5]. As only one antenna is active at each time instant, the ICI problem is avoided. Also, as only one RF chain is needed, the overall system complexity is greatly reduced, and transmit power consumption is much lower [6]. Benefiting from this, SM has the potential to be used for massive MIMO systems [7].

The performance of SM systems so far has only been investigated over simple fixed-to-vehicle (F2V) channels, such as Rayleigh, Rician, and Nakagami channels [3], [5–7]. However, communication environments will be more complex under V2V scenarios due to high mobility. Various of statistical properties of V2V channels have been investigated in [9–12]. To the best of authors' knowledge, the BER performance of SM systems under V2V channels has not been studied yet. To fill the aforementioned gap, this paper derives the theoretical BER expression of SM systems under V2V channels, and study the impact of some key V2V channel parameters, such as the maximum Doppler frequencies at both the Tx and Rx, on statistical properties of V2V channels, and the performance of SM systems [8].

The rest of the paper is organized as follows. In Section II, a general introduction of SM systems is given. In Section III, the V2V channel model is investigated. The theoretical BER expression of SM systems under V2V channels is derived in Section IV. In Section V, simulation results of SM systems under V2V channel models are presented. Finally, conclusions are given in Section VI.

II. Spatial Modulation

The block diagram of the SM simulator under V2V channels is shown in Fig. 1. In SM, the transmitted data bits at a particular time instant are used to activate a single transmit antenna among the set of N_T transmit antennas and mapped to one constellation symbol of M-QAM/PSK constellation diagrams. For instance, a mapping table for a SM system considering two transmit antennas and BPSK modulation is shown in Table. I. The spectral efficiency of a SM, in the unit of bits/symbol, therefore, given as

$$m = \log_2(N_T) + \log_2(M) \ . \tag{1}$$

978-1-4799-4482-8/14/$31.00 ©2014 IEEE

In Table I, two data bits ($m = 2$) are transmitted at each time instant using BPSK modulation and two transmit antennas. The spectral efficiency of SM can be improved by increasing the number of transmit antennas. This is one reason why SM can be used for massive MIMO systems.

TABLE I
SM MAPPING TABLE FOR $N_T = 2$ AND $M = 2$.

Input Bits	Antenna Index	Transmit Symbol
00	1	+1
01	1	-1
10	2	+1
11	2	-1

The transmitted vector $s(t)$ at each particular time instant from the multi transmit antennas contains only one non-zero symbol. The vector is transmitted over the MIMO channel matrix $H(t,\tau)$ with $N_r \times N_t$ dimension where N_r denotes the number of receive antennas. Thus, the signal vector received at the receiver can be written as

$$y(t) = H(t,\tau) \otimes S(t) + n(t)\,. \tag{2}$$

Here, $H(t,\tau)$ is the channel matrix composed of $h_{p,q}(t)$ which denotes the complex fading envelope between the p_{th} Tx and the q_{th} Rx antenna elements, $S(t)$ is the transmitted vector, $n(t)$ is the complex additive white Gaussian noise (AWGN) vector with real and imaginary parts both having a double-sided power spectral density equal to $N_0/2$ [5], and $\otimes$ is the convolution operator.

The receiver's task is to jointly estimate the active transmit antenna index and the transmitted symbol at this particular time instant. The optimum ML detector is assumed with perfect time synchronization and full channel state information (CSI) at the receiver aims to jointly estimate the transmit antenna index $\hat{p}$ and the transmitted data symbol $\hat{s}_k$ that minimize the following metric

$$\begin{aligned} &[\hat{p}, \hat{s}_k] = \arg\min_{p,k} \left(\|y - HS\|_F^2 \right) \\ &p \in \{1 : N_t\} \text{ and } k \in \{1 : M\} \end{aligned} \tag{3}$$

where $\|\cdot\|_F$ denotes the Frobenius norm of a matrix.

III. VEHICLE-TO-VEHICLE CHANNEL SIMULATOR

Recently, several theoretical channel models have been proposed for MIMO V2V channels under non-isotropic scattering environments [8], [10]. To implement these theoretical channel models, corresponding simulation models which assume finite number of effective scatterers are needed. Among various simulation models, the deterministic sum-of-sinusoids (SoS) simulation model has been widely used due to its lower complexity and acceptable accuracy. In this paper, a widely used two-ring deterministic SoS simulation model [9], [11] is applied. In this model, we suppose there are N_1 and N_2 effective scatterers around the Tx and Rx and lying on two rings of radii R_T and R_R, respectively. The distance between the Tx and Rx is D. The antenna element spacings at the Tx and Rx are δ_T and δ_R, respectively. The reasonable assumptions $\min\{R_T, R_R\} \gg \max\{\delta_T, \delta_R\}$ and $D \gg \max\{\delta_T, \delta_R\}$ are used here. The multi-element antenna tilt angles are β_T and β_R. The Tx and Rx move with speeds υ_T and υ_R in directions determined by the angles of motion γ_T and γ_R, respectively. The angle of arrival (AoA) of the waves traveling from an effective scatterer at the Rx ring towards the Rx is denoted by $\tilde{\phi}_R^{(n_2)}$ ($n_2 = 1, ..., N_2$) and the angle of departure (AoD) of the waves that impinge on an effective scatterer at the Tx ring is designated by $\tilde{\phi}_T^{(n_1)}$ ($n_1 = 1, ..., N_1$). Therefore, the complex fading envelope between the p_{th} Tx and the q_{th} Rx antenna elements can be expressed as [11]

$$\begin{aligned} \tilde{h}_{p,q}(t) = \sum_{n_1,n_2=1}^{N_1,N_2} \frac{1}{\sqrt{N_1 N_2}} e^{j2\pi f_{T_{\max}} t \cos(\tilde{\phi}_T^{(n_1)} - \gamma_T)} \\ \times e^{j\left[2\pi f_{R_{\max}} t \cos(\tilde{\phi}_R^{(n_2)} - \gamma_R) \tilde{\psi}_{n_1,n_2} - 2\pi f_c \tau_{p,q,n_1,n_2}\right]} \end{aligned} \tag{4}$$

where f_c denotes the carrier frequency, $f_{T_{\max}} = (\upsilon_T/c) f_c$ and $f_{R_{\max}} = (\upsilon_R/c) f_c$ are the maximum Doppler frequency of the Tx and Rx, respectively, with c being the speed of light. In (4), $\tilde{\psi}_{n_1,n_2}$ denotes the phase, which is assumed as a uniform distributed random variable within $[-\pi, \pi)$, and $\tau_{p,q,n_1,n_2} = (\varepsilon_{pn_1} + \varepsilon_{n_1 n_2} + \varepsilon_{n_2 q})/c$ is the travel time of the waves from the Tx to the Rx with $\varepsilon_{pn_1} \approx R_T - k_p \delta_T \cos(\tilde{\phi}_T^{(n_1)} - \beta_T)$, $\varepsilon_{n_2 q} \approx R_R - k_q \delta_R \cos(\tilde{\phi}_R^{(n_2)} - \beta_R)$, and $\varepsilon_{n_1 n_2} \approx D$, where $k_p = M_T - 2p + 1/2$ and $k_q = M_R - 2q + 1/2$.

The von Mises distribution [10] is applied to model the distributions of AoA and AoD and has the following expression as $f(\phi) \triangleq \exp[k\cos(\phi - \mu)]/[2\pi I_0(k)]$, where μ is the mean value of angles and k denotes the angular spread. Applying the von Mises distribution, we can have the distribution of the AoA and AoD as $f\left(\tilde{\phi}_R\right) \triangleq \exp[k_R \cos(\phi_R - \mu_R)]/[2\pi I_0(k_R)]$ and $f\left(\tilde{\phi}_T\right) \triangleq \exp[k_T \cos(\phi_T - \mu_T)]/[2\pi I_0(k_T)]$, respectively, where $\tilde{\phi}_R$ and $\tilde{\phi}_T$ are the continuous expressions of the discrete AoA $\tilde{\phi}_R^{(n_2)}$ and AoD $\tilde{\phi}_T^{(n_1)}$, respectively.

The sets of AoA $\tilde{\phi}_R^{(n_2)}$ and AoD $\tilde{\phi}_T^{(n_1)}$ are obtained through the newly proposed parameter computation method in [11]. For the sake of brevity, this method is not explained here and the reader is referred to [11] for more details.

The space-time correlation function of this deterministic SoS channel simulator can be obtained from

$$\tilde{\rho}_{\tilde{h}_{pq}\tilde{h}_{p'q'}}(\tau) = \left\langle \tilde{h}_{pq}(t) \tilde{h}^*_{p'q'}(t-\tau) \right\rangle \tag{5}$$

where $\langle\cdot\rangle$ denotes the time average operator.

IV. THEORETICAL ANALYSIS

The theoretical BER of SM system can be approached through the union bound method [13]. Related investigations have been published in [5]- [6] and [13]- [14]. In [7], an improved union bound is presented. It classified all errors into 3 types, which are expressed as:

$$\underset{SM}{ABER} \leqslant \underset{Signal}{ABER} + \underset{Spatial}{ABER} + \underset{Joint}{ABER}\,. \tag{6}$$

In (6), $\underset{Signal}{ABER}$ denotes how the performance of SM is purely affected by signal constellation schemes, which means errors only occur in the part of information carried by modulation symbols. In [7], the $\underset{Signal}{ABER}$ is defined as:

$$\underset{Signal}{ABER} = \frac{1}{N_t}\frac{\log_2(M)}{m}\sum_{n_t=1}^{N_t} APEB_{MOD}(n_t) \tag{7}$$

where

$$\underset{MOD}{APEB}(n_t) = \frac{1}{M}\frac{1}{\log_2(M)} N_H\left(\chi \to \tilde{\chi}\right) P(\chi \to \tilde{\chi}) \ . \tag{8}$$

In (8), $N_H\left(\chi \to \tilde{\chi}\right)$ is the hamming distance between χ and $\tilde{\chi}$, which is expressed as e in following equations, $P(\chi \to \tilde{\chi})$ denotes the pairwise error probability (PEP) of χ is decided to $\tilde{\chi}$ by mistake. For different modulation schemes, their BER expression have been investigated in [7], [13] and [16]. Using M-PSK as an example, (8) can be expressed as [7]

$$\begin{aligned}\underset{MOD}{APEB}(n_t) = \frac{1}{\log_2(M)}\sum_{l=1}^{M-1}\Bigg[\Bigg(2\left|\frac{l}{M} - \left\lfloor\frac{l}{M}\right\rfloor\right| \\ + 2\sum_{k=2}^{\log_2(M)}\left|\frac{l}{2^k} - \left\lfloor\frac{l}{2^k}\right\rfloor\right|\Bigg)\Bigg] P_l(n_t)\end{aligned} \tag{9}$$

where

$$\begin{aligned}P_l(n_t) = &\int_0^{\pi[1-(2l-1)/M]} M_r\left(2SNR\frac{\sin^2\left[\pi(2l-1)/M\right]}{\sin^2\theta}\right)d\theta \\ &- \int_0^{\pi[1-(2l+1)/M]} M_r\left(2SNR\frac{\sin^2\left[\pi(2l+1)/M\right]}{\sin^2\theta}\right)d\theta.\end{aligned} \tag{10}$$

In (10), $M_r(s)$ is the moment generation function (MGF) of $\sum_{l=1}^{N_r}\left|h_{n_t,l}\right|^2$, which can be expressed as:

$$M_r(s) = \prod_{i=1}^{N_R}\left(1 - s\lambda_i e\right)^{-1}. \tag{11}$$

In (11), λ_i is the eigenvalue of receivers correlation indicator R_{Rx}, similarly, we can define R_{Tx} as the correlation indicator of transmitters with the eigenvalue u_j. For our channel model, these two parts are expressed as:

$$R_{Tx}(p,\tilde{p}) = \rho_{h_{p,q}h_{\tilde{p},q}}(0), R_{Rx}(q,\tilde{q}) = \rho_{h_{p,q}h_{p,\tilde{q}}}(0) \tag{12}$$

where $\rho_{h_{p,q}h_{\tilde{p},q}}(.)$ is the STCFs of the V2V channel. The theoretical BER of information carried by the index of antennas is presented by $\underset{Spatial}{ABER}$, which is defined as:

$$\underset{Spatial}{ABER} = \frac{1}{M}\frac{\log_2(N_t)}{m}\sum_{l=1}^{M}\underset{SSK}{APEB}(l) \tag{13}$$

In (13), $\underset{SSK}{APEB}(l)$ can be expressed as [16]:

$$\begin{aligned}\underset{SSK}{APEB}(l) = \frac{1}{N_t}\frac{1}{\log_2(N_t)}\sum_{n_t=1}^{N_t}\sum_{\tilde{n}_t=1}^{N_t}\Bigg[N_H\left(n_t \to \tilde{n}_t\right) \\ \times\frac{1}{\pi}\int_0^{\pi/2} M_{n_t,\tilde{n}_t}\left(\frac{SNR\times\kappa_l^2}{2\sin^2\theta}\right)d\theta\Bigg]\end{aligned} \tag{14}$$

where $M_{n_t,\tilde{n}_t}(.)$ is the MGF of the random variable $\sum_{l=1}^{N_r}\left|h_{n_t,l} - h_{\tilde{n}_t,l}\right|^2$. Based on investigations of [15], the close-form expression of the MGF can be written as:

$$M_{n_t,\tilde{n}_t}(s) = \prod_{j=1}^{N_T}\prod_{i=1}^{N_R}\left(1 - s\lambda_i u_j\right)^{-1} \tag{15}$$

The $\underset{Joint}{ABER}$ indicates the joint effect of previous two elements. In [16], it is defied as:

$$\begin{aligned}\underset{Jo\,\mathrm{int}}{ABER} = \frac{1}{N_t M}\frac{1}{m}\sum_{n_t=1}^{N_t}\sum_{\tilde{n}_t\neq n_t=1}^{N_t}\left[N_H\left((n_t,\chi)\to(\tilde{n}_t,\tilde{\chi})\right)\right. \\ \left.\times P\left((n_t,\chi_l)\to(\tilde{n}_t,\tilde{\chi}_l)\right)\right]\end{aligned} \tag{16}$$

where

$$P\left((n_t,\chi)\to(\tilde{n}_t,\tilde{\chi})\right) = \frac{1}{\pi}\int_0^{\frac{\pi}{2}} M_{\alpha_{n_t\chi,\tilde{n}_t\tilde{\chi}}}\left(\frac{SNR}{2\sin^2\theta}\right)d\theta \ . \tag{17}$$

In (17), $M_{\alpha_{n_t\chi,\tilde{n}_t\tilde{\chi}}}(.)$ is the MGF of $\sum_{l=1}^{N_r}\left|h_{n_t,l}\chi - h_{\tilde{n}_t,l}\tilde{\chi}\right|^2$. Its close-form expression can be obtained from [15] as

$$M_{\alpha_{n_t\chi,\tilde{n}_t\tilde{\chi}}}(s) = \prod_{j=1}^{N_T}\prod_{i=1}^{N_R}\left(1 - s\lambda_i e u_j\right)^{-1}. \tag{18}$$

V. Simulation Results

In this section, the effect of different channel configurations on the channel's statistic property and the performance of the SM system will be investigated. Unless further specified, the simulation is configured with the following parameters: $f_c = 5.9$ GHz, $f_{T_{\max}} = f_{R_{\max}} = 570$ Hz, $\beta_T = \beta_R = \gamma_T = \gamma_R = 50^\circ$, $D = 300$ m, $R_T = R_R = 12$ m, $k = 1$, and $N_1 = N_2 = 30$, 16-QAM will be used as the default modulation scheme except the theoretical derivation part. In this work, following the LTE standard, the bandwidth of the system is configured as 1.4MHz, with the corresponding sampling rate of 1.92MHz.

The channel model's STCF under different antenna spacing settings are shown in Fig. 2. Obtained simulation results are in perfect match with the theoretical ones, which validates the simulation model and the following simulations. Also, the absolute value of STCF decreases with increasing distance between different antenna elements.

The effect of maximum Doppler frequencies and antenna spacing settings on the absolute values of the channel's STCFs are illustrated in Fig. 3. It is noticed that the STCFs vary significantly for different Doppler values (which correspond to different speeds of movement). Besides, it is shown that

with larger Doppler frequencies (which means higher speed movement), the fading period of the channel becomes shorter, which indicates that the channel becomes worse. It is necessary to mention that when $f_{T_{\max}} = 0$, the channel can be treated as a F2V scenario.

Theoretical and simulation results for BER performance of SM under V2V channel models with different antenna spacing settings are compared in Fig. 4. It is necessary to indicate that all results are obtained using QPSK modulation scheme. From Fig. 4, our theoretical derivation is shown to be able to get reasonable accuracy, theoretical curves can fit simulation results well, especially in high SNR part.

The BER performance affected by different modulation schemes and antenna spacing settings. It can be observed that the SM system will have better BER performance when using lower order modulation. Also, larger antenna spacings will lead to lower spatial correlation and consequently better BER performance. This viewpoint can be proved by Fig. 2 as well, which indicates how the STCF is affected by the antenna spacing setting.

The effect of the maximum Doppler frequency which corresponds to the movement speed, on the BER performance of SM systems is depicted in Fig. 6. We can find that lower speed will result in better performance. Comparing F2V with V2V scenarios at the same $f_{R_{\max}}$, it can be concluded that under the same antenna spacing setting, SM system has better performance with the F2V scenario. However if we compare the case of $f_{T_{\max}} = 0, f_{R_{\max}} = 570Hz$ with $f_{T_{\max}} = f_{R_{\max}} = 190Hz$, we find that even the second case is V2V scenario, its performance is still better than the F2V case with higher absolute speed. Thus, a significant conclusion is drawn that the absolute speed between Tx and Rx has stronger impact on the BER performance than the change in the scenario itself.

The effect of the distance between Tx and Rx on the BER performance is investigated in Fig. 7. Longer distances decrease the reliability of SM system. Though, it has been improved in [11] that the STCF is not affected by the distance between Tx and Rx. Hence, the degradation of SM performance with larger Tx-Rx distance is not due to the increase in channel correlation, but is caused by the significant loss of power as the result of path loss effect.

VI. Conclusions

In this paper, we have investigated the BER performance of SM systems over V2V channel models by theoretical analysis and simulations. The impact of different propagation characteristics, e.g., antenna element spacings, maximum Doppler frequency, and Tx-Rx distance, on the correlation properties of V2V channels and BER performance of SM systems have been analyzed.

Acknowledgements

The authors would like to acknowledge the support of this work from the International Science & Technology Cooperation Program of China (No. 2014DFA11640), the Opening Project of the Key Laboratory of Cognitive Radio and Information Processing (Guilin University of Electronic Technology), Ministry of Education (Grant No.: 2013KF01), SNCS research center at University of Tabuk under the grant from the Ministry of Higher Education in Saudi Arabia, the Fundamental Research Program of Shenzhen City (No. JCYJ20120817163755061 and JC201005250067A), and National Natural Science Foundation of China (No. 61372077 and 61101079).

References

[1] C.-X. Wang, X. Hong, X. Ge, X. Cheng, G. Zhang, and J. S. Thompson, " Cooperative MIMO channel models: a survey," *IEEE Commun. Mag.*, vol. 48, no. 2, pp. 80–87, Feb. 2010.

[2] E. Telatar, "Capacity of Multi-Antenna Gaussian Channels," *European Transaction Telecommunication*, vol. 10, no. 6, pp. 558–595, November,1999.

[3] J. Jeganathan, A. Ghrayeb, and L. Szczecinski, "Spatial modulation: optimal detection and performance analysis," *IEEE Commun. Lett.,* vol. 12, no. 8, pp. 545–547, Aug. 2008.

[4] G. J. Foschini, "Layered space-time architecture for wireless communication in a fading environment when using multi-element antennas," *Bell Labs Tech. J.,* vol. 1, no. 2, pp. 41–59, Sep. 1996.

[5] R. Mesleh, H. Haas, and S. Sinanovic, "Spatial modulation," *IEEE Trans. Veh. Technol.,* vol. 57, no. 4, pp. 2228–2241, Jul. 2008.

[6] J. Jeganathan, A. Ghrayeb, and A. Ceron, "Space shift keying modulation for MIMO channels," *IEEE Trans. Wireless Commun.*, vol. 8, no. 7, pp. 3692–3703, Jul. 2009.

[7] M. D. Renzo and H. Haas, "Bit Error Probability of SM-MIMO Over Generalized Fading Channels," *IEEE Trans. Veh. Technol.*, vol. 61, no. 3, pp. 1124–1144, Mar. 2012.

[8] C.-X. Wang, X. Cheng, and D. I. Laurenson, "Vehicle-to-vehicle channel modeling and measurements: recent advances and future challenges," *IEEE Commun. Mag.*, vol. 47, no. 11, pp. 96–103, Nov. 2009.

[9] C. S. Patel, G. L. Stüber, and T. G. Pratt, "Simulation of Rayleigh faded mobile-to-mobile communication channels," *IEEE Trans. Commun.*, vol. 53, no. 11, pp. 1876–1884, Nov. 2005.

[10] X. Cheng, C.-X. Wang, D. I. Laurenson, S. Salous, and A. V. Vasilakos, "An adaptive geometry-based stochastic model for non-isotropic MIMO mobile-to-mobile channels," *IEEE Trans. Wireless Commun.*, vol. 8, no. 9, pp. 4824–4835, Sept. 2009.

[11] X. Cheng, Q. Yao, C.-X. Wang, B. Ai, G. L. Stüber, D. Yuan, and B. Jiao, "An improved parameter computation method for a MIMO V2V Rayleigh fading channel simulator under non-isotropic scattering environments," *IEEE Commun. Lett.* , vol. 17, no. 2, pp. 265–268, Feb. 2013.

[12] X. Cheng, Q. Yao, M. Wen, C.-X. Wang, L. Song, and B. Jiao, "Wideband channel modeling and ICI cancellation for vehicle-to-vehicle communication systems," *IEEE J. Sel. Areas Commun.*, vol. 31, no. 9, pp. 434–448, Sept. 2013.

[13] M. K. Simon and M.-S. Alouini, *Digital Communication over Fading Channels.* , 2nd edition, John Wiley & Sons, 2005.

[14] M. Di Renzo and H. Haas, "A general framework for performance analysis of space shift keying (SSK) modulation for MISO correlated Nakagami-m fading channels," *IEEE Trans. Commun.*, vol. 58, no. 9, pp. 2950–2603, Sept. 2010.

[15] A. Hedayat, H. Shah, and A. Nosratinia, "Analysis of space-time coding in correlated fading channels," *IEEE Trans. Wireless Commun.* , vol. 4, no. 6, pp. 2882–2891, Nov. 2005.

[16] M.-S. Alouini,and A. J. Goldsmith, "A unified approach for calculating the error rates of linearly modulated signals over generalized fading channels," *IEEE Trans. Commun.*, vol. 47, no. 9, pp. 1324–1334, Sept. 1999.

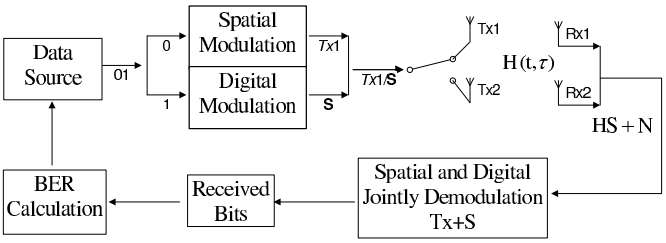

Fig. 1. Block diagram of the SM system.

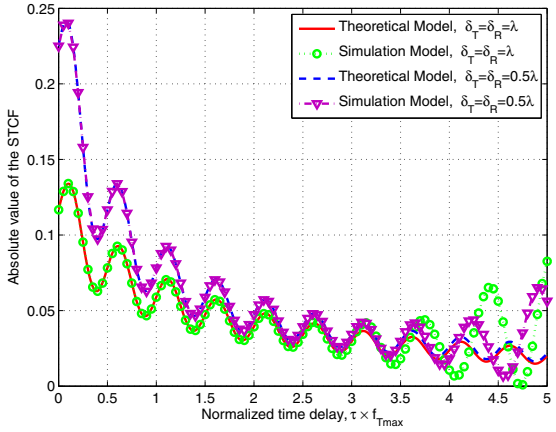

Fig. 2. Absolute values of STCFs for theoretical and simulation V2V MIMO channel models with different antenna spacings.

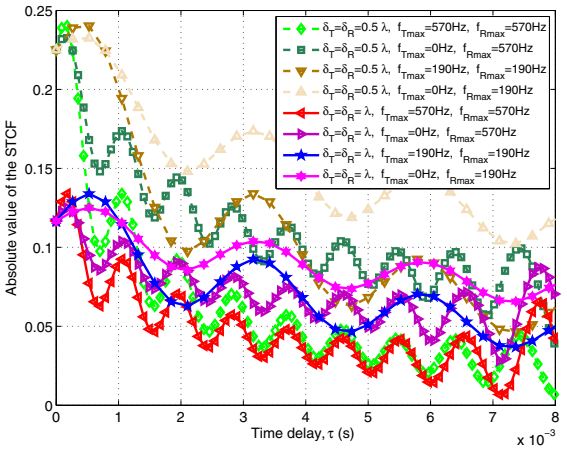

Fig. 3. Absolute values of STCFs for the V2V MIMO channel simulator with different Doppler frequencies.

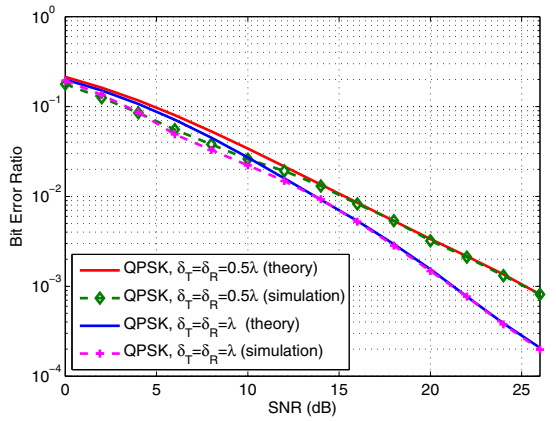

Fig. 4. Comparison between theoretical and simulation results of BER performance for SM systems over the V2V MIMO channel models.

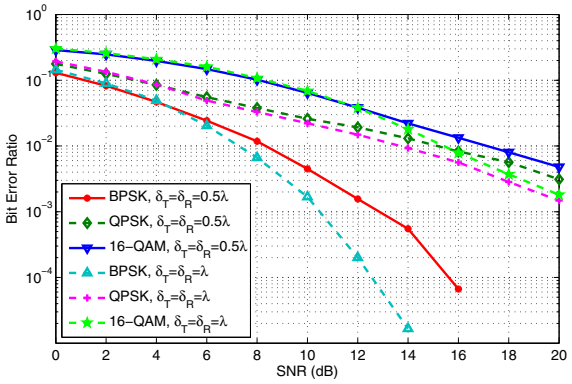

Fig. 5. BER versus the SNR for the SM system with different modulation schemes and antenna spacings.

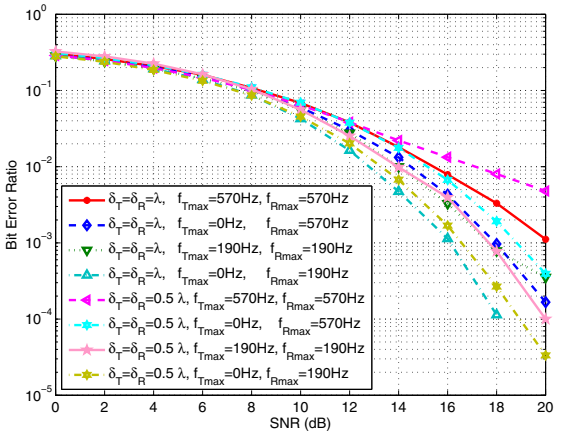

Fig. 6. BER versus the SNR for the SM system with different maximum Doppler frequencies of the Tx and Rx.

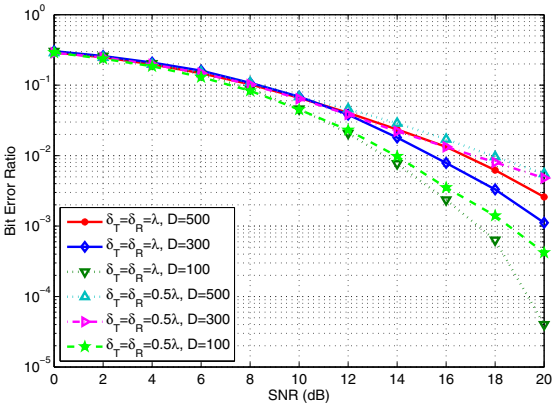

Fig. 7. BER versus the SNR for the SM system with different distances between the Tx and Rx.